Electromagnetic Shielding Performance of Nickel Plated Expanded Graphite/Wood Fiber Composite

Yi Chen,[a,b] Chuwang Su,[a,b,*] Quanping Yuan,[a,b] Manjun Zhan,[c] Bing Yang,[a,b] and Junwei Xia [a,b]

To develop a wood-based electromagnetic shielding composite, *in-situ* electroless plating was used to plate nickel onto the surface of expanded graphite (EG) to obtain nickel-plated EG (Ni-EG), and the Ni-EG was mixed with wood fiber to manufacture the composite. The optimal plating formula was as follows: 20 g/L $NiSO_4 \cdot 6H_2O$ as the main salt, 60 g/L $N_2H_4 \cdot H_2O$ as the reducing agent, 50 g/L $Na_3C_6H_5O_7 \cdot 2H_2O$ as the complexing agent, 40 g/L $CH_3COONa \cdot H_2O$ as the buffering agent, pH value 11, and a temperature of 90 °C. These conditions yielded the highest quality of nickel coating (3.57 g). As EG concentration increased from 2 to 10 g/L, the percentage of the Ni-EG in the composite was 60%, the thickness of the composite was 2 mm, the density was 0.9 g/cm^3, the magnetic properties and resistivity of the Ni-EG decreased from 29.5 to 5.57 emu/g and 80.2 to 10.7 mΩ·cm, respectively, and the electromagnetic shielding effectiveness (SE) and the reflectivity of the composite increased from 55 to 60 dB and −3.6 to -1.8 dB, respectively. Consequently, the introduction of nickel is suitable for improving the absorbing performance of Ni-EG/wood fiber composites, leading to better SE in a broad frequency range.

Keywords: Expanded graphite; Chemical nickel plating; Wood fiber; Shielding effectiveness; Reflectivity

Contact information: a: Forestry College of Guangxi University, Nanning 530004, P. R. China; b: Key Laboratory of Guangxi Colleges and Universities for Forestry Science and Engineering, Nanning 530004, P. R. China; c: Guangxi Fenglin Forest Industry Co., Ltd., Nanning 530221, P. R. China;
** Corresponding author: glscw58@163.com*

INTRODUCTION

With the rapid development of science and technology, a variety of electronics have been widely used, which has resulted in electromagnetic interference among electronics and electromagnetic radiation pollution in the environment (Ahuja *et al.* 1999). Electromagnetic shielding materials that absorb and reflect electromagnetic waves can reduce these hazards (Kim *et al.* 2005; Xu *et al.* 2010). Among them, wood-based electromagnetic shielding composites have become a trend in this type of composite because of their desirable properties, such as reproducibility, natural degradability, and natural aesthetics. As a common preparation method, electroless plating is used to coat a layer of metal onto the wood surface to make the composite. Exhibiting good electromagnetic shielding effectiveness (SE), electroless nickel plating on wood surfaces (Huang 2005; Wang *et al.* 2005; Huang and Zhao 2006) and electroless copper plating (Li *et al.* 2014) have been investigated in many studies. To improve the SE and mechanical performance of the coating layer, researchers (Hui *et al.* 2014) successfully plated a Ni-Cu-P alloy layer on a wood veneer. It had a SE between 55 and 60 dB in the frequency range of 9 kHz to 1.5 GHz.

Because of the secondary pollution of electromagnetic wave as the common shielding composite used, electromagnetic wave absorbing materials have been drawing more attention (Qin and Brosseau 2012). As the important parameter for evaluating and enhancing absorbing performance, complex permittivity and permeability can also be studied to simulate the wave reflectivity of composites (Christian and Philippe 2005; Brosseau *et al.* 2008). In order to improve absorbing performance of the common carbonaceous shielding material, some function material with good electromagnetic properties such as magnetic metal material (Lozano *et al*. 2009), ferrite material (Yusoff and Abdullah 2004), helical chiral material (Sun *et al.* 2000), and polymer material (Gnidakouong *et al.* 2013) could be adopted to fill in its micropore or coat on its surface; this topic is becoming a new study direction.

Furthermore, for the development of integrally conductive filled-type wood-based electromagnetic shielding composite with good attenuation performance, metal membrane (Lu *et al*. 2011), metal powders (Liu and Fu 2009), metal mesh (Zhang *et al.* 2004; Liu *et al.* 2010; Su *et al*. 2013), carbon black, carbon fiber (Hou *et al.* 2015), or plated carbon fiber (Yuan *et al.* 2013), carbon fiber paper (Yuan *et al*. 2014), and even mineral powder with excellent electromagnetic properties (Su *et al*. 2012) can be mixed or laminated with wood material to manufacture wood composites with high conductivity and high shielding effectiveness. Wood-based electromagnetic shielding composites have excellent characteristics, but also some limitations, such as high density of the composite with metal filler, complicated construction, and the fact that the texture is too hard to mold. On the other hand, surface electroless plating focuses on the reflecting-type wood-based electromagnetic shielding composite which cannot be used for situations demanding low reflection and high absorption. Therefore, research on composites with light, process-able, and wide-band electromagnetic shielding is practical and promising (Yavuz *et al.* 2005; Yu and Shen 2009).

Because of the increasingly urgent need for high comprehensive shielding performance with reflection and absorption, and especially good compatibility with wood material, more and more carbon material has been used in wood functional composites. Expanded graphite (EG), which is composed of flake graphite, has good properties, such as low density, flexibility, and good thermal and chemical stability. However, there has not been much research about wood-based electromagnetic shielding composites made with the EG. Moreover, microholes in EG result in a situation where incident EM waves are repeatedly reflected at different directions on its surface or in the holes, which make it conducive to attenuation for electromagnetic waves (Maiti *et al.* 2013). Furthermore, its vermicular shape (appears to be a fiber shape) can contribute to mixing with other components uniformly (Kratochvíla *et al*. 2013). When the vermicular EG is mixed with wood fiber to make a composite, it will form a three-dimensional conductive net structure with more interspaces among EG, similar to that of the composite with carbon fiber (Hou *et al*. 2015), which is helpful for the multiple reflection and attenuation. Also, wood-based composite is friendlier to the environment compared with metal or high polymer-based material. However, its electromagnetic shielding effectiveness is not good at low frequencies because of its diamagnetic properties (Huang *et al.* 2007). To improve broadband shielding functionality, especially absorption attenuation, magnetic metal materials should be evenly loaded on the surface to regulate the relationship between electrical properties and magnetic properties and give the composite a strong electrical conductivity and magnetic permeability at the same time (Ren *et al*. 2009), which is also the problem of this study to solve.

Consequently, in this study, flake graphite was used to make lightweight EG; then, nickel, a magnetic metal, was coated onto the surface of EG by electroless plating to improve its magnetic permeability. The plated EG was also mixed with wood fiber to prepare a homogeneous and lightweight nickel-plated EG/wood fiber electromagnetic shielding composite with broadband shielding.

EXPERIMENTAL

Materials

Flake graphite with an ash content ≤ 8% was purchased from Qingdao Jin Rilai Graphite Co., Ltd. in China. Eucalyptus and pine hybrid wood fibers (moisture content 9% to 11%) were offered by Guangxi Fenglin Forest Industry Co., Ltd. in China. Isocyanate adhesive (concentration 100%) was purchased from Shanghai Huntsman Polyurethane Co., Ltd. in China. Other chemicals used in the experiments are shown in Table 1.

Table 1. Chemical Reagents for Testing

No.	Chemicals
1	$C_4H_6O_4Ni \cdot 4H_2O$
2	$NaBH_4$
3	$N_2H_4 \cdot H_2O$
4	$Na_3C_6H_5O_7 \cdot 2H_2O$
5	$CH_3COONa \cdot H_2O$
6	$NiSO_4 \cdot 6H_2O$

Note: The chemical reagents were all analytically pure.

Methods

Orthogonal experiment for nickel plating on EG

EG was homemade by a two-step acidification and oxidation method (Zhao *et al*. 2014) and its expansion rate is more than 200. The microstructure of EG was analyzed using a scanning electron microscope (SEM, S-3400N, Hitachi, Japan).

Ni-EG was manufactured with the EG by the following steps. In the beginning, 500 mL of 8 g/L $C_4H_6O_4Ni \cdot 4H_2O$ and 7 g/L $NaBH_4$ were taken separately, and 10 g of EG was put into the $C_4H_6O_4Ni \cdot 4H_2O$ solution to soak for 10 min. Then the $NaBH_4$ solution was slowly added to the mixture mentioned above and left to stand until air bubbles stopped being generated. After that, the solution was filtered with a suction filter (SHZ-D, Shanghai Ziqi Laboratory Equipment Co., Ltd., China). Finally, the solid and filter paper were placed in a vacuum drying oven (ZKGT-6050, Shenzheng Aodema Electronic Technology Co., Ltd., China) to dry. An initial Ni-EG could be obtained after this step.

Afterwards, 2 g of the initial Ni-EG was put into a beaker. Successively, 20 g of $NiSO_4 \cdot 6H_2O$, 50 to 70 g of $N_2H_4 \cdot H_2O$, 40 to 60 g of $Na_3C_6H_5O_7 \cdot 2H_2O$ and 30 to 50 g of $CH_3COONa \cdot H_2O$ was added into the beaker, and the corresponding volume of water was poured into the beaker to make the concentration of plating solution according to the test design in Table 2. An orthogonal test $L_9(3^3)$ with three impact factors and three levels was used to optimize the plating solution formula, in which the impact factors included the concentrations of $N_2H_4 \cdot H_2O$, $Na_3C_6H_5O_7 \cdot 2H_2O$, and $CH_3COONa \cdot H_2O$. The concentration

of $NiSO_4 \cdot 6H_2O$ was set at 20 g/L based on preliminary tests, by which the initial concentration of Ni^{2+} was more proper. And the final concentration of EG was 2 g/L.

Also, 4 mol/L of NaOH was used to adjust pH value of the solution in the range from 10 to 13. Then, the beaker was placed in a water bath (HHSII-1, Shanghai Wujiu Automation Equipment Co., Ltd., China), and the temperature was set at 80 to 95 °C. At the same time, an electric blender (JJ-1 500W, Hengshui Jinhai Chemical Instrument Co., Ltd., China) was used to stir the solution at 100 rpm until air bubbles stopped evolving. Finally, the solution was filtered with a suction filter, and the solid and filter paper were dried in a vacuum drying oven. The microstructure and elementary composition of Ni-EG were analyzed using SEM and energy dispersive spectroscopy (EDS; XM260S, Hitachi, Japan). The electrical resistivity and hysteresis loop of Ni-EG were analyzed using a four-point probe (ST2258C, Suzhou Jingge Electronic Co., Ltd., China) and vibrating sample magnetometer (VSM; 7410, Lake Shore, USA).

Table 2. Design for Orthogonal Test L_9 (3^3)

No.	(A) $N_2H_4 \cdot H_2O$ (g/L)	(B) $Na_3C_6H_5O_7 \cdot 2H_2O$ (g/L)	(C) $CH_3COONa \cdot H_2O$ (g/L)
1	50	40	30
2	60	50	40
3	70	60	50

Single-factor experiment for nickel plating with various pH and temperature values

The effect of temperature and pH on coating quality was studied using the single-factor analysis method. The pH values were set to 10, 11, 12, and 13 by using the above solution of NaOH. The temperature was set to 80, 85, 90, and 95 °C. The solution concentrations of the chemical plating bath were the same as the optimal formula determined in the orthogonal test.

Single-factor experiment for nickel plating with various concentrations of EG

In this single-factor experiment, the amount of EG was changed for plating, and Ni-EG with various conductivities and magnetic properties was finally prepared. The optimal formula of the electroless plating solution, pH, and temperature, determined from the previous experiment, were used. The concentration of EG was set to 2, 4, 6, 8, and 10 g/L; the corresponding serial number of the Ni-EG as 1#, 2#, 3#, 4# and 5#, respectively.

Preparation of Ni-EG/wood fiber composite

The Ni-EG and wood fiber were used to manufacture composites. First, the wood fiber was put into a blender with isocyanate adhesive, then mixed with Ni-EG evenly. The composite was prepared by mat formation, preloading, and the hot pressing process. The plate blank was preloaded with a flat vulcanizing machine (XLBIOO-D, Qingdao Yiming Rubber & Machinery Co., Ltd., China) under a pressure of 2.8 MPa for 10 min. The hot press conditions were as follows: a plate temperature of 160 °C, a duration of 10 min, and a pressure of 3.5 MPa.

The main factors affecting SE were percentage of Ni-EG, thickness and density of the composite, and type of Ni-EG (Table 3). The single-factor analysis method was used to optimize the four factors.

First, the thickness, density of the composite, and type of Ni-EG were set at 3 mm, 0.7 g/cm^3, and 1# Ni-EG, respectively. The percentage of Ni-EG was set at 30%, 40%,

50%, 60%, and 70%. Second, the density, percentage of Ni-EG, and type of Ni-EG were set at 0.7 g/cm^3, 60 %, and 1# Ni-EG, respectively, and the thicknesses of the composites were 1, 2, and 3 mm. Third, the thickness, percentage of Ni-EG, and type of Ni-EG were set at 2 mm, 60%, and 1# Ni-EG, respectively, and the densities of the composites were 0.7, 0.8, 0.9, and 1.0 g/cm^3. Finally, the thickness, density, and percentage of Ni-EG were set at 2 mm, 0.9 g/cm^3, and 60%, and the types of Ni-EG used were 1#, 2#, 3#, 4#, and 5#, respectively.

After the composites with different formulas were prepared, their microstructures, elementary compositions, SE, and reflectivity was analyzed using SEM, EDS, layout of the flange coaxial test device (DR-02, Beijing Dingrong EMC Technology Company, China), and the plate material reflectivity test system (home-made by the University of Electronic Science and Technology, China).

Calculation of plating quality

Plating quality was calculated based on Eq. 1,

$$M_c = (M_{\mathrm{EG2}} + M_{\mathrm{L2}}) - (M_{\mathrm{EG1}} + M_{\mathrm{L1}}) \quad (1)$$

where M_{EG1} is the mass of EG, M_{EG2} is the mass of Ni-EG after drying, M_{L1} is the mass of the filter paper, and M_{L2} is the mass of the filter paper after drying.

SEM and EDS analysis

Samples of EG and Ni-EG were taken in powder form. They were each mounted on a stub with double-sided conductive tape. The micro-structures of EG and Ni-EG were observed using a scanning electronic microscope with EDS (S-3400N, Hitachi, Japan) operating at an accelerating voltage of 20 kV.

Magnetic test method

A vibration sample magnetometer (VSM, 7410, Lakeside Temperature Company, USA) was used to measure the coercive force of EG and Ni-EG hysteresis. Powder samples of the EG and Ni-EG weighed less than 50 mg. The testing range was between −10000 and 10000 Oe.

Electrical resistivity testing method

After the Ni-EG powder was formed into a 50 mm × 50 mm × 2 mm slab, a four-point probe resistivity tester (ST2258C, Suzhou Lattice Electronic Co., Ltd., China) was used to test the resistivity of five points on the sample slab, and the average was taken. Four replicate specimens of each type were measured.

SE testing method

According to the Chinese standard SJ 20524 (1995), composites were cooled for 24 h, then formed into disc specimens of diameter $115^{0}_{-0.5}$ mm. The SE of the composites was tested using a DN15115 type vertical flange coaxial test device (developed by Southeast University of China). Three replicate specimens of each type were prepared and tested. The frequency range for testing SE was 100 to 1500MHz.

SE was divided into the following grades (Zhao 2001): under 10 dB, no effectiveness; 10 to 30 dB, bad; 30 to 60 dB, medium; 60 to 90 dB, good; and above 90 dB,

excellent. Among them, composite materials of medium grade could be used for general industrial and commercial electronic equipment.

Reflectivity testing method

According to the Chinese standard GJB 2038 (1994), the composite was cooled for 24 h, then cut into 200 mm × 200 mm × 2 mm slabs. The test frequency range was between 2 and 18 GHz. The reflectivity of the composite was tested using the plate material reflectivity test system. Completion of the testing was entrusted to the University of Electronic Science and Technology in China.

RESULTS AND DISCUSSION

Analysis of the Process for Nickel Plating on EG

In the electroless nickel plating orthogonal experiment, the highest plating quality was identified as the objective function. Data processing for the electroless nickel plating orthogonal experiment is shown in Table 3.

Table 3. Results of the Orthogonal Experiment

No.	$N_2H_4 \cdot H_2O$ (g/L)	$Na_3C_6H_5O_7 \cdot 2H_2O$ (g/L)	$CH_3COONa \cdot H_2O$ (g/L)	Coating Quality (g)
1	50	40	30	2.91
2	50	50	40	3.01
3	50	60	50	2.97
4	60	40	40	3.18
5	60	50	50	3.24
6	60	60	30	3.14
7	70	40	50	2.87
8	70	50	30	3.12
9	70	60	40	3.02
K1	8.89	8.96	9.17	
K2	9.56	9.37	9.21	
K3	9.01	9.13	9.08	
k1	2.96	2.99	3.06	
k2	3.19	3.12	3.07	
k3	3.00	3.04	3.03	
R	0.22	0.14	0.04	

Note: K is the sum of experimental result (coating quality) of each factor in the same level. k is the average value of corresponding K. R is range of k, *i.e*. the difference between maximum and minimum of k value.

Based on the results of the factor analysis chart in Fig. 1, the factors ordered from strongest effect to weakest effect were $N_2H_4 \cdot H_2O$ > $Na_3C_6H_5O_7 \cdot 2H_2O$ > $CH_3COONa \cdot H_2O$. The best formulas were $Na_3C_6H_5O_7 \cdot 2H_2O$ at 50 g/L, $N_2H_4 \cdot H_2O$ at 60 g/L, and $CH_3COONa \cdot H_2O$ at 40 g/L. The mechanism for the electroless plating nickel can be seen in Fig. 2, where nickel would continually deposit in the vicinity of the nickel absorbed on the EG in the preprocess after the plating initiated.

The reduction ability of plating solution was enhanced as the concentration of $N_2H_4 \cdot H_2O$ increased, which enabled the reaction to occur more easily (Bulasara *et al*. 2012). In this study, 60 g/L of its concentration was more proper.

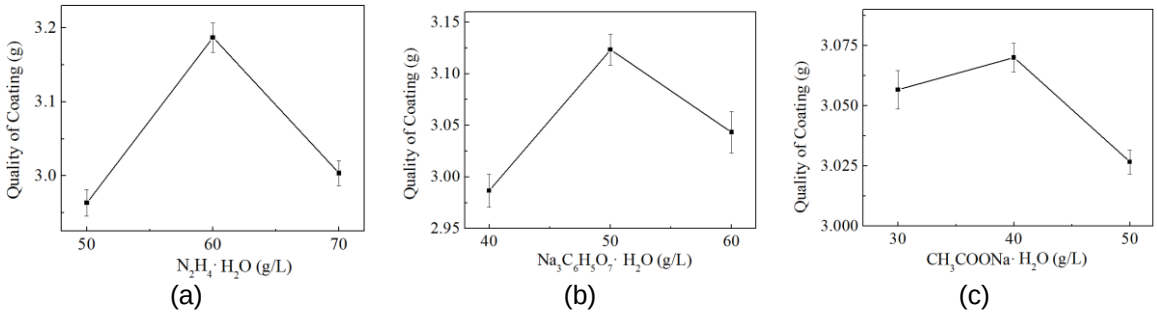

Fig. 1. Relationship between coating quality and factors

In addition, as the concentration of $Na_3C_6H_5O_7 \cdot 2H_2O$ reached 50 g/L, Ni^{2+} under an appropriate concentration could form clathrate with that, which have improved the deposition rate. What is more, $CH_3COONa \cdot H_2O$ as a pH regulator prevented the solution from reacting too drastically. As its concentration of 40 g/L was used, the plating solution was more stable and nickel could more easily deposit onto the EG.

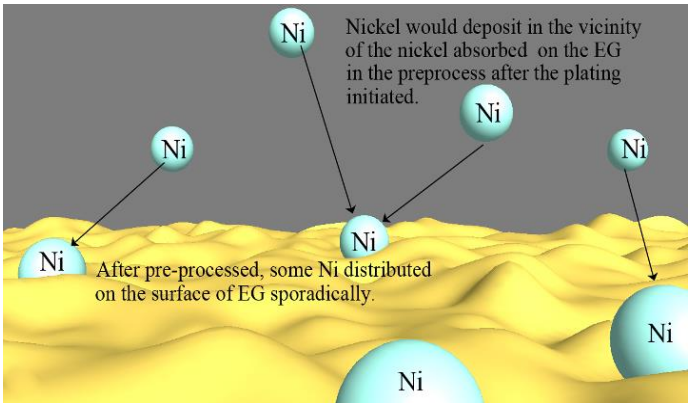

Fig. 2. Schematic diagram of *in-situ* electroless plating

Analysis of the Performance of Nickel Plating with Various pH Values and Temperatures

With $N_2H_4 \cdot H_2O$ as a reducing agent, chemical nickel plating proceeded under alkaline conditions, so the coating deposition rate could be improved effectively as the pH increased. It can be seen in Fig. 3 that a pH of 11 was most conducive to improving coating quality and yielded a coating of 3.5 g.

The optimum temperature was 90 °C, as can be seen in Fig. 4; the reaction rate and deposition rate of nickel were both enhanced, as the activity of Ni^{2+} was greatly increased at this temperature. However, the coating quality slightly decreased at 95 °C because the activity of Ni^{2+} was too high, which resulted in the low deposition of nickel.

The optimal formula for nickel plating EG was $NiSO_4 \cdot 6H_2O$ at 20 g/L, $N_2H_4 \cdot H_2O$ at 60 g/L, $Na_3C_6H_5O_7 \cdot 2H_2O$ at 50 g/L, $CH_3COONa \cdot H_2O$ at 40 g/L, pH value 11, and a temperature of 90 °C; this resulted in the highest coating quality (3.57 g/L of plating solution).

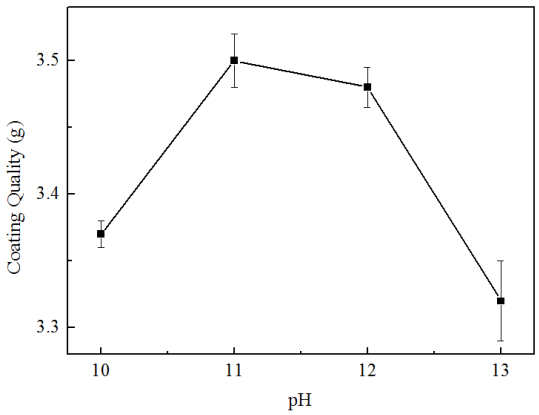

Fig. 3. Influence of pH on coating quality

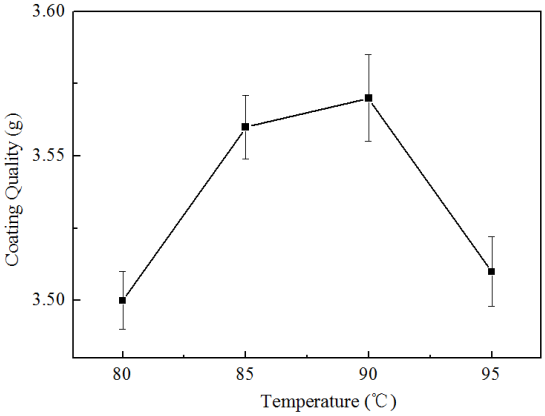

Fig. 4. Influence of temperature on coating quality

It can be seen from the SEM of EG in Fig. 5(a) that there were many holes on the surface of EG, which allowed the nickel to be easily deposited onto the surface. The results of the SEM and EDS area scanning of Ni-EG in Figs. 5(b) and (c) showed that nickel coated the surface of EG uniformly and also showed high quality when using the optimal formula.

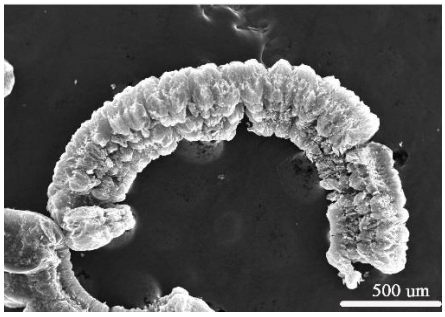

(a) SEM of EG

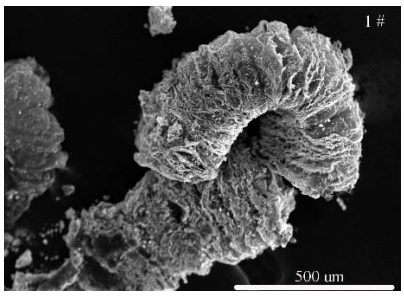

(b) SEM of Ni-EG

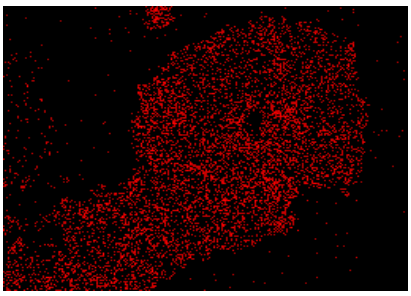

(c) EDS area scanning of Ni-EG

Fig. 5. SEM and EDS analysis of EG before and after plating

Electromagnetic Performance for Nickel Plating with Various Concentrations of EG

Resistivity of Ni-EG

The resistivity of EG is 10.1 mΩ·cm lower than that of nickel, so the conductivity of Ni-EG primarily depends on the content of EG (Dhakate *et al*. 2008). The resistivity of Ni-EG made with various concentrations of EG is shown in Fig. 6. The resistivity declined

with increasing EG concentration. Among them, the resistivity of 1# Ni-EG was 80.2 mΩ·cm, then 5# Ni-EG decreased to 10.7 mΩ·cm, which is close to that of pure EG.

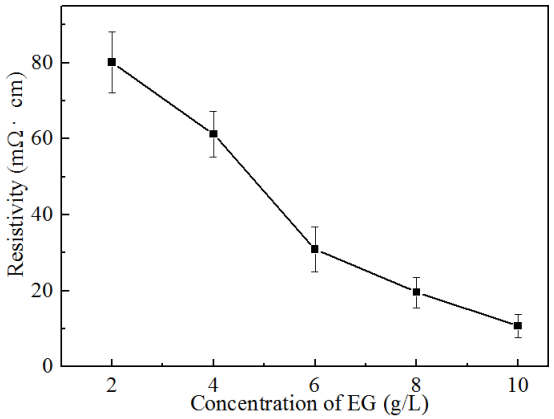

Fig. 6. Resistivity of Ni-EG made with various concentrations of EG

Moreover, the change in resistivity was also verified by the results shown in Figs. 7 to 12, in which SEM and EDS analysis of various Ni-EG formulations is shown. The elemental analysis diagram for 1# Ni-EG is shown in Fig. 7. There were three kinds of main elements: N, O, and C. The quality fraction of nickel was 61.13 wt.%. The O element came from the remaining −OH in the process of nickel plating and a small amount of oxidized nickel generated in the drying process.

Figures 8 to 12(a) and (b) show the SEM and EDS area scanning analysis for t Ni-EG, respectively. Area scanning of the nickel element on 1 to 5# Ni-EG showed that nickel on the surface of EG decreased when the concentration of EG increased. The red points on Figs. 8 to 12(b) represent the nickel elements, and their distribution density and uniformity was used to determine the quality and uniformity of the coating. The difference of the area scanning results between 1 and 5# Ni-EG was obvious. 1# Ni-EG had more nickel on its surface, so its conductivity was relatively lower. The results demonstrated that the introduction of nickel has a negative influence on the conductivity of EG.

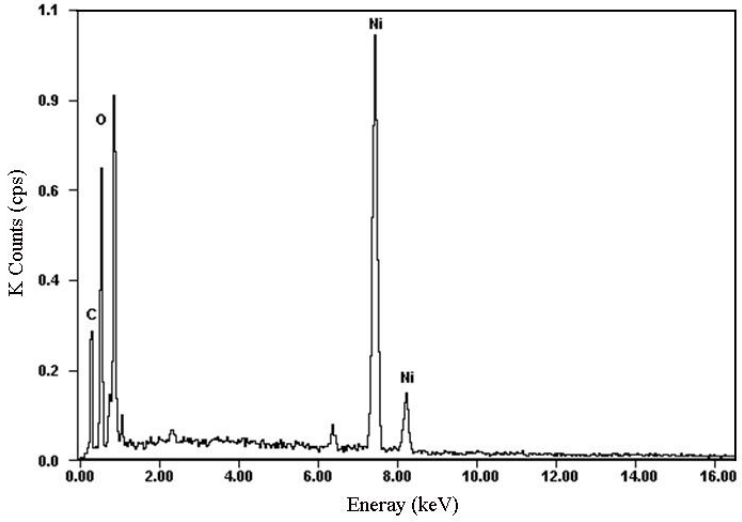

Fig. 7. EDS chemical element analysis of 1# Ni-EG

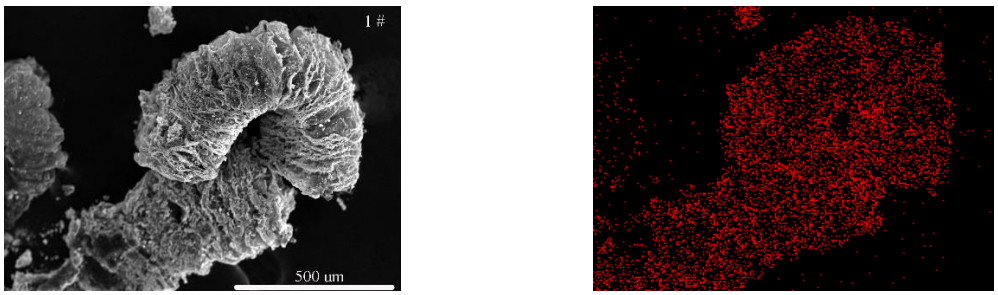

(a) (b)

Fig. 8. SEM and EDS of 1# Ni-EG

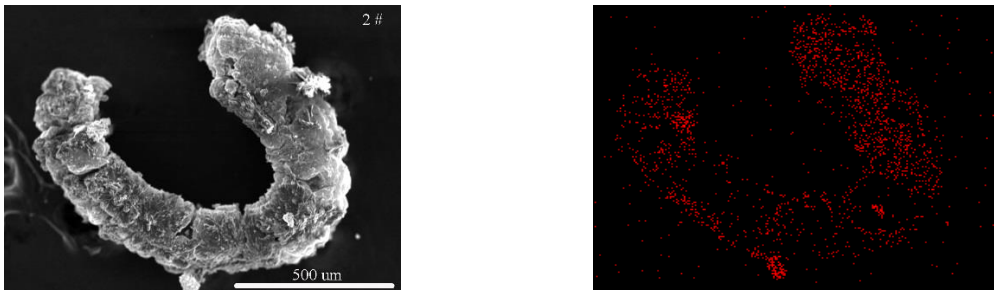

(a) (b)

Fig. 9. SEM and EDS of 2# Ni-EG

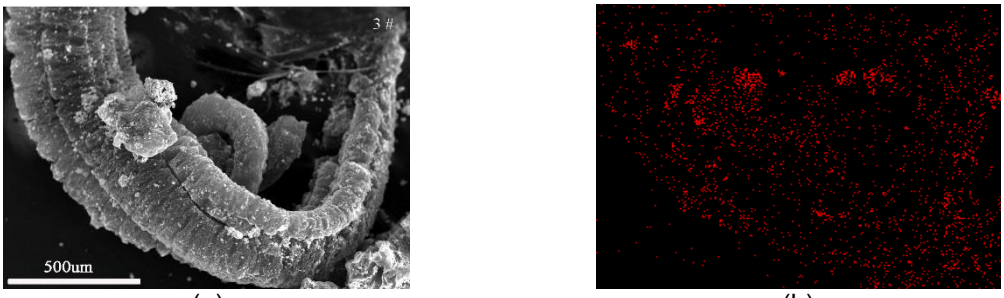

(a) (b)

Fig. 10. SEM and EDS of 3# Ni-EG

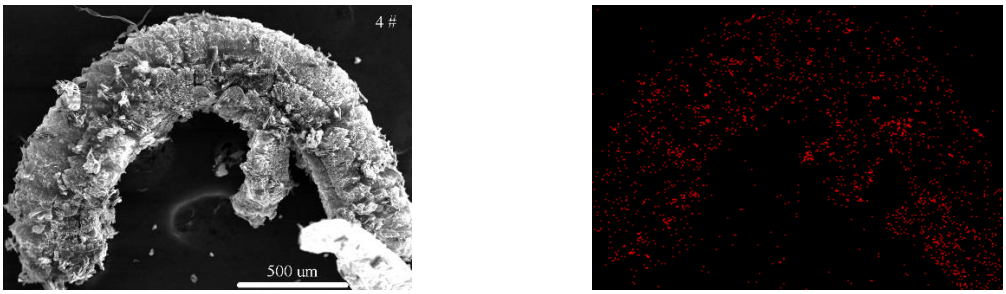

(a) (b)

Fig. 11. SEM and EDS of 4# Ni-EG

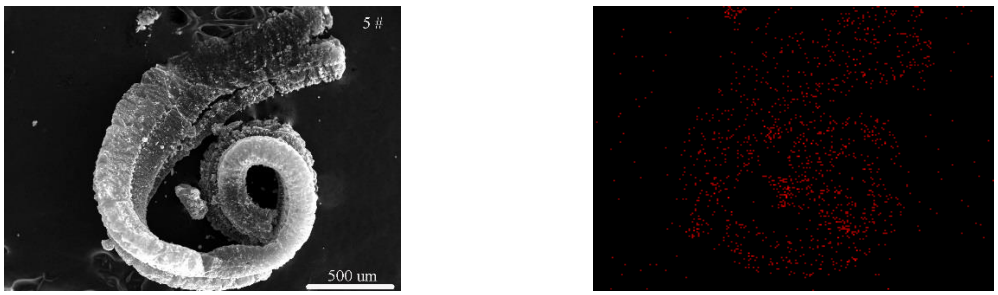

(a) (b)

Fig. 12. SEM and EDS of 5# Ni-EG

Magnetics of Ni-EG

The hysteresis loops of Ni-EG made with various concentrations of EG are shown in Fig. 13. The saturation magnetization and coercive force are shown in Fig. 14. The hysteresis loops appeared slender, and the coercive force was very low, which indicated that the Ni-EG would demagnetize quickly and conform to the characteristics of the soft magnetic material. As the amount of nickel on EG decreased, the saturation magnetization decreased. 1# Ni-EG's saturation magnetization was 29.5 emu/g, while that of 5# Ni-EG was only 5.57 emu/g. However, the coercive force changed differently because the anisotropy, particle size, and flaws of the material were different. Coercive force had less influence on the magnetism of the materials. Consequently, the results above demonstrated that nickel coating is conducive to improving the magnetism of Ni-EG and even its composites (Polák and Petráš 2015).

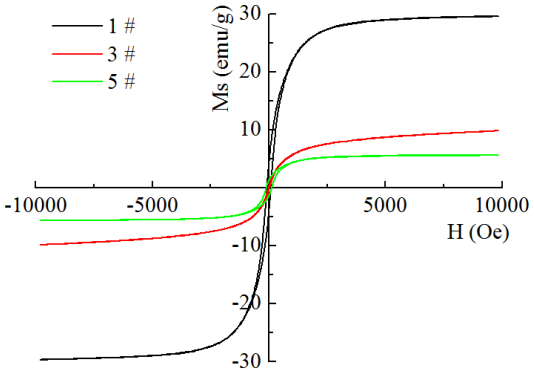

Fig. 13. Hysteresis loop of Ni-EG made with different concentrations of EG

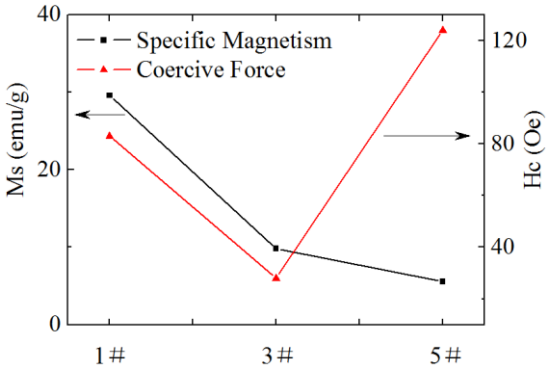

Fig. 14. Saturation magnetization and coercive of Ni-EG made with different concentrations of EG

Electromagnetic Shielding Efficiency of the Composite

The SE of Ni-EG/wood fiber composites with various contents of Ni-EG is shown in Fig. 15(a). In order to reveal the limit value with content of Ni-EG, the average SE value in the range from 100 to 1500 MHz is exhibited in Fig. 15(b). When the percentage of Ni-EG was higher than 60 %, the SE changed slightly and remained at approximately 40 dB in the range of 100 to 1500 MHz. When the Ni-EG content was low, the spacing distance between Ni-EG particles was large and tunnels conducting by the way of electronic transition could not form, which affected the SE. Therefore, the filling quantity had to reach

the percolation threshold to promote the formation of the tunnel conductive circuit net (Kim *et al.* 2004).

The SE of Ni-EG/wood fiber composites with various thicknesses is shown in Fig. 16(a). The average SE range of 100 to 1500 MHz is shown in Fig. 16(b). When the thickness reached 2 mm or higher, there was not much more addition of SE, which could be seen as the limit value. Under the effect of the alternating magnetic field of electromagnetic waves, eddy current and magnetic loss around nickel with high magnetism were generated by the magnetic induction function. At the same time, a magnetic field in the opposite direction of the extra magnetic field was generated by the eddy current, which weakened the function of the magnetic field in the interior of the composite and decayed the intensity of the magnetic field inside the material exponentially, producing a skin effect. For highly conductive EG, extra alternating current resulted in the instability of its internal current and caused the current to concentrate on its surface (skin effect). Therefore, the composite should not be too thick.

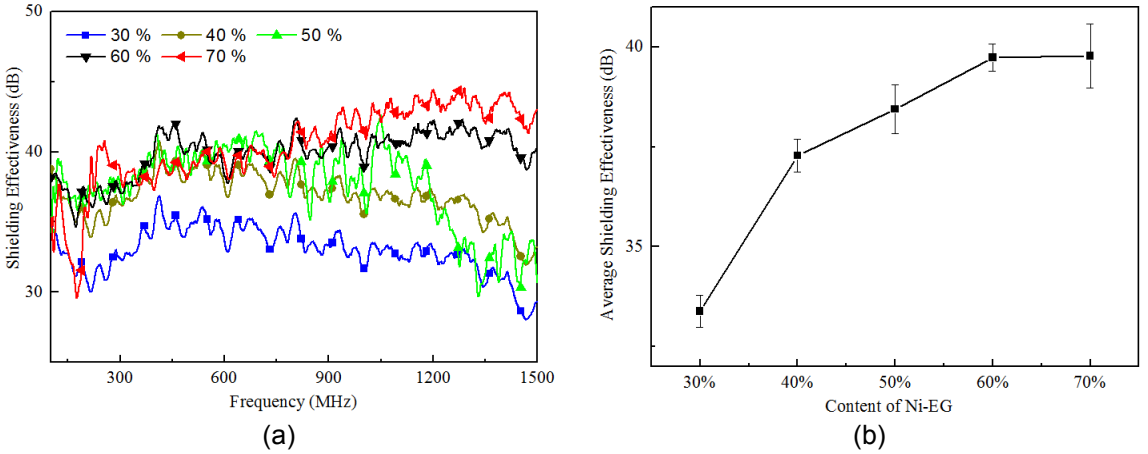

Fig. 15. SE of Ni-EG/wood fiber composites with different contents of Ni-EG

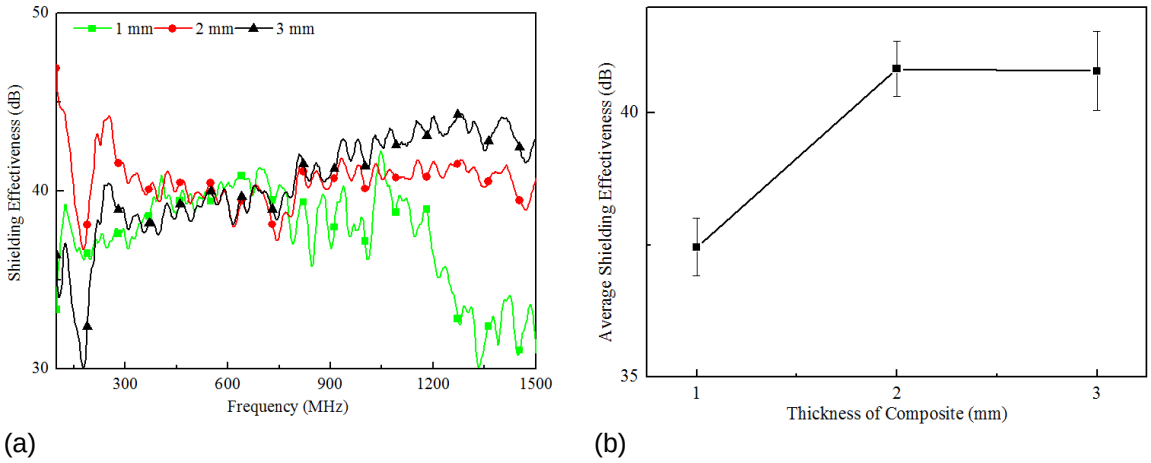

Fig. 16. SE of Ni-EG/ wood fiber composites with different thicknesses

Figure 17(a) shows that the average SE of Ni-EG/wood fiber composites with various densities was approximately 60 dB in the range of 100 to 1500 MHz, as the density of the composite board reached 0.9 g/cm^3 or above. And the average SE range of 100 to

1500 MHz is shown in Fig. 17(b). The density change of the composite had a noticeable effect on SE. Increased density caused the distance between Ni-EG particles to shorten; then, the conductive mode increasingly changed from tunnel conduction to contact conduction. The current generated from the extra electric field became larger and the dielectric loss was enhanced, which improved SE.

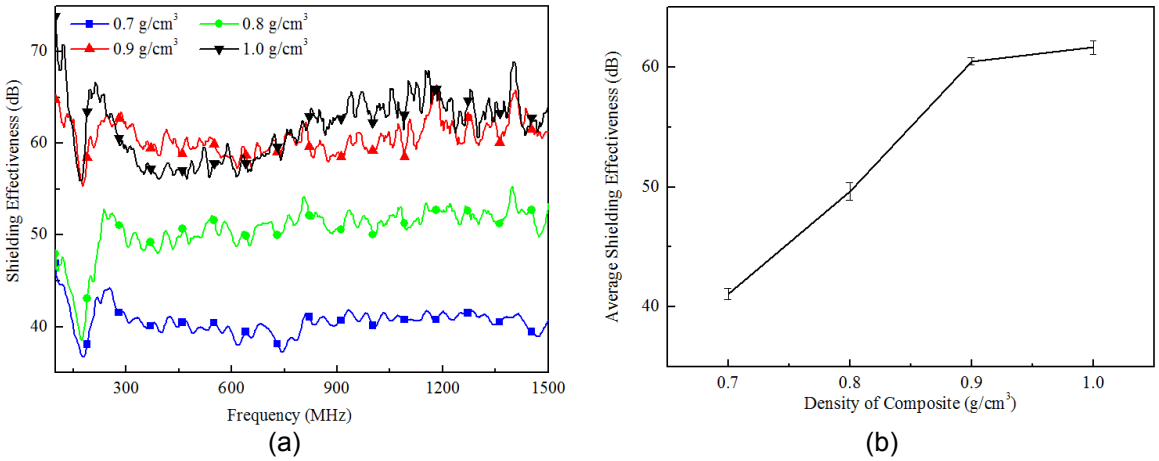

Fig. 17. SE of Ni-EG/wood fiber composites with various densities

The SE of Ni-EG/wood fiber composites with 1#~5# Ni-EG are shown in Fig. 18. Among them, the nickel content of 1# Ni-EG was the highest. From 1# to 5# composites, the content of nickel decreased. That is to say, the magnetism of the composite decreased and the conductivity increased. Even so, SE increased. Moreover, the density of nickel was higher than that of EG and the volume of EG was higher than that of nickel at the same quality. Then volume of EG in the composite increased from 1# to 5#. Consequently, Ni-EG particles were contacted more closely after the composite was manufactured with the same density, thickness, and percentage of Ni-EG, which greatly improved its SE, *i.e.*, the composite with 5# Ni-EG had the highest SE (higher than 60 dB) in the range of 100 to 1500 MHz.

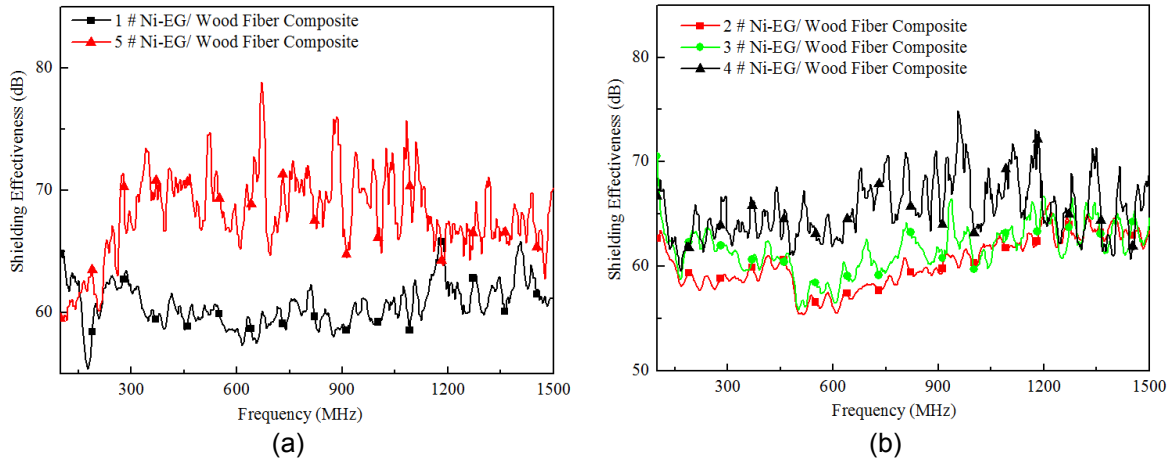

Fig. 18. SE of Ni-EG/wood fiber composite with 1#~5# Ni-EG

In summary, when the type of Ni-EG, percentage of Ni-EG, thickness, and density of the composite were set to 5#, 60 %, 2 mm, and 0.9 g/cm^3, respectively, the composite had the highest SE (higher than 60 dB) in the range of 100 to 1500 MHz.

Reflectivity of the Composite

The complex permittivity and complex permeability of EG are both low, so it has almost no loss function for electromagnetic waves. However, nickel has a high complex permeability and could therefore absorb electromagnetic waves. As the content of nickel in the composite increased, the peak of reflectivity decreased (as the value decreased, the ability to absorb electromagnetic waves improved). The reflectivity of 1# and 5# Ni-EG/wood fiber composites when the percentage of Ni-EG, thickness, and density of the composite were set to 60 %, 2 mm, and 0.9 g/cm^3, respectively, is shown in Fig. 19. Both types of composites had a peak in the range of 9.5 GHz, but the peak of 1# Ni-EG/wood fiber composite was −3.6 dB, which was less than −1.8 dB in the peak of 5# Ni-EG/wood fiber composite.

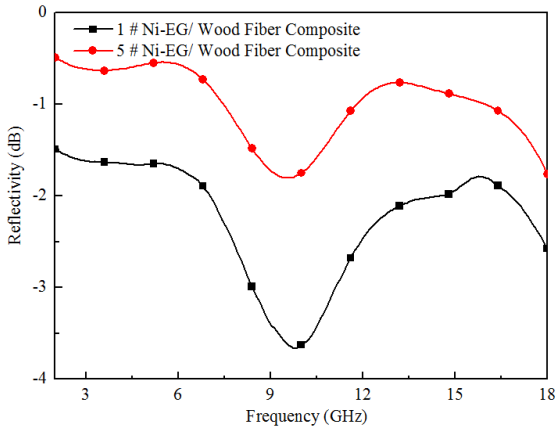

Fig. 19. Reflectivity of Ni-EG/wood fiber composite with 1 # and 5 # Ni-EG

CONCLUSIONS

1. The optimal formula and processing conditions for electroless nickel plating on EG were $N_2H_4 \cdot H_2O$ at 60 g/L, $NiSO_4 \cdot 6H_2O$ at 20 g/L, $Na_3C_6H_5O_7 \cdot 2H_2O$ at 50 g/L, $CH_3COO\ Na \cdot H_2O$ at 40 g/L, pH 11, and a temperature of 90 °C, which yielded a nickel coating quality of 3.57 g/L of plating solution.
2. 1# Ni-EG made with a 2 g/L concentration of EG had a higher electromagnetic performance, *i.e.*, a magnetic property of 29.5 emu/g, and a resistivity of 80.2 mΩ·cm. However, the magnetic property and resistivity of 5# Ni-EG made with a 10 g/L concentration of EG was 5.57 emu/g and 10.7 mΩ·cm, respectively. Results showed that higher EG concentrations yielded a lower nickel coating quality of Ni-EG and a better conductivity of Ni-EG, but the magnetic properties declined slightly.
3. When the type of Ni-EG, percentage of Ni-EG, and thickness and density of the composite were set at 5#, 60 %, 2 mm, and 0.9 g/cm^3, respectively, the composite had a better SE (higher than 60 dB) in the range of 100 to 1500 MHz, but the reflectivity was only −1.8 dB in the range of 2 to 18 GHz. When the type of Ni-EG was 1#, the SE of the composite was higher than 55 dB and the reflectivity was −3.6 dB. The results

indicated that the introduction of nickel is conducive to improving the absorbing performance of Ni-EG/wood fiber composite and it has better SE in a broad frequency range.

ACKNOWLEDGMENTS

This work was partially supported by the Guangxi Provincial Scientific Research Foundation (No. 14122005-37) and the Innovation Project of Guangxi Graduate Education (No. YCSZ2015052). The authors are grateful to the Scientific Agency of Guangxi Province and the Education Agency of Guangxi Province for the financial support of this work.

REFERENCES CITED

Ahuja, Y. R., Jahan, P., and Bhargava, S. C. (1999). "Epidemiological and laboratory studies on the cancer risk from electromagnetic fields: An overview," *Proceeding of the International Conference on Electromagnetic Interference and Compatibility*, December 6-8, New Delhi, India, pp. 459-464.

Brosseau, C., Mdarhri, A., and Vidal, A. (2008). "Mechanical fatigue and dielectric relaxation of carbon black/polymer composites," *Journal of Applied Physics* 104(7), 074105. DOI: 10.1063/1.2988269

Bulasara, V. K., Uppaluri, R., and Purkait, M. K. (2012). "Effect of ultrasound on the performance of nickel hydrazine electroless plating baths," *Materials and Manufacturing Processes* 27(2), 201-206. DOI: 10.1080/10426914.2011.566663

Christian, B., and Philippe, T. (2005). "Instrumentation for microwave frequency-domain spectroscopy of filled polymers under uniaxial tension," *Measurement Science & Technology* 16(9), 1823-1832. DOI: 10.1088/0957-0233/16/9/015

Dhakate, S. R., Sharma, S., Borah, M., Mathur, R. B., and Dhami, T. L. (2008). "Development and characterization of expanded graphite-based nanocomposite as bipolar plate for polymer electrolyte membrane fuel cells (PEMFCs)," *Energy & Fuels* 22(5), 3329-3334. DOI: 10.1021/ef800135f

GJB 2038 (1994). "Methods for measurement of reflectivity of radar absorbing material," China Commission of Science Technology and Industry for National Defense, Beijing, China.

Gnidakouong, J. R. N., Kim, M., Park, H. W., Park, Y. B., and Jeong, H. S. (2013). "Electromagnetic interference shielding of composites consisting of a polyester matrix and carbon nanotube-coated fiber reinforcement," *Composites Part A Applied Science & Manufacturing* 50(7), 73-80. DOI: 10.1016/j.compositesa.2013.03.007

Hou, J. F., Fu, F., Lu, K. Y., and Chen, L. Z. (2015). "Highly conductive fiberboards made with carbon and wood fibers," *BioResources* 10(4), 6348-6362. DOI: 10.15376/biores.10.4.6348-6362

Huang, J. T. (2005). "The effect of plating solution composition on wood electroless nickel plating depositing rate," *Journal of Inner Mongolia Agricultural University (Natural Science Edition)* 26(1), 57-60. DOI: 10.3969/j.issn.1009-3575.2005.01.015

Huang, J. T., and Zhao, G. J. (2006). "Effects of technological parameters on nickel deposition rate on wood by electroless plating method," *China Wood Industry* 20(1), 15-17. DOI: 10.3969/j.issn.1001-8654.2006.01.005

Huang, Y., Xu, Z., Shen, J., Tang, T., and Huang, R. (2007). "Dispersion of magnetic metals on expanded graphite for the shielding of electromagnetic radiations," *Applied Physics Letters* 90(13), 133117. DOI: 10.1063/1.2718269

Hui, B., Li, J., and Wang, L. (2014). "Electromagnetic shielding wood-based composite from electroless plating corrosion-resistant Ni-Cu-P coatings on *Fraxinus mandshurica* veneer," *Wood Science and Technology* 48(5), 961-979. DOI: 10.1007/s00226-014-0653-0

Kim, H., Kim, M. K., Lee, C. Y., Joo, J., Cho, S. J., Yoon, H. S., and Epstein, A. J. (2004). "Electrical conductivity and electromagnetic interference shielding of multiwalled carbon nanotube composites containing Fe catalyst," *Applied Physics Letters* 84(4), 577-589. DOI: 10.1063/1.1641167

Kim, S. S., Kim, S. T., Yoon, Y. C., and Lee, K. S. (2005). "Magnetic, dielectric and microwave absorbing properties of iron particles dispersed in rubber matrix in gigahertz frequencies," *Journal of Applied Physics* 97, 10F905. DOI: 10.1063/1.1852371

Kratochvíla, J., Boudenne, A., and Krupa, I. (2013). "Effect of filler size on thermophysical and electrical behavior of nanocomposites based on expanded graphite nanoparticles filled in low-density polyethylene matrix," *Polymer Composites* 34(2), 149-155. DOI: 10.1002/pc.22387

Li, C. Q., Wang, S. C., and Zhou, Y. F. (2014). "Study on manufacture of copper coated expanded graphite," *Journal of Heilongjiang University of Science and Technology* 24(5), 500-502. DOI: 10.3969/j.issn.2095-7262.2014.05.013

Liu, X. M., and Fu, F. (2009). "Study on performance of electro-conductive powder and veneer composite," *Journal of Nanjing Forestry University (Natural Science Edition)* 33(2), 95-98. DOI: 10.3969/j.issn.1000-2006.2009.02.023

Liu, H., Li, J., and Wang, L. (2010). "Electroless nickel plating on APTHS modified wood veneer for EMI shielding," *Applied Surface Science* 257(4), 1325-1330. DOI: 10.1016/j.apsusc.2010.08.060

Lozano, K., Espinoza, L., Hernandez, K., Adhikari, R., and Radhakrishnan, G. (2009). "Investigation of the electromagnetic interference shielding of titanium carbide coated nanoreinforced liquid crystalline polymer," *Journal of Applied Physics* 105(10), 103511. DOI: 10.1063/1.3130397

Lu, K. Y., Fu, F., Cai, Z. Y., Fu, Y. J., and Zhang, Y. M. (2011). "Study of properties of electromagnetic shielding plywood laminated with conductive sheets," *Journal of Building Materials* 14(2), 207-211. DOI: 10.3969/j.issn.1007-9629.2011.02.012

Maiti, S., Shrivastava, N. K., Suin, S., and Khatua, B. B. (2013). "Polystyrene/MWCNT /graphite nanoplate nanocomposites: Efficient electromagnetic interference shielding material through graphite nanoplate–MWCNT–graphite nanoplate networking," *ACS Applied Materials & Interfaces* 5(11), 4712-4724. DOI: 10.1021/am400658h

Polák, J., and Petráš, R. (2015). "Hysteresis loop analysis in cyclically strained materials," *Advanced Structured Materials* 57, 185-205. DOI: 10.1007/978-3-319-14660-7_10

Qin, F. X., and Brosseau, C. (2012). "A review and analysis of microwave absorption in polymer composites filled with carbonaceous particles," *Journal of Applied Physics* 111(6), 061301. DOI: 10.1063/1.3688435

Ren, Q. F., Jia, Y., and Zhang, Q. Y. (2009). "Property of electroless nickel plating on expanded graphite," *Chinese Journal of Applied Chemistry* 26(4), 495-497. DOI: 10.3969/j.issn.1000-0518.2009.04.029

SJ 20524 (1995). "Measuring methods for shielding effectiveness of materials," The Ministry of Industrial Electronics of The People's Republic of China, Beijing, China.

Su, C. W., Yuan, Q. P., Gan, W. X., Dai, D., Huang, J., and Huang, Y. (2012). "Study on a composite fiberboard with multiple electromagnetic shielding effectiveness," *The Open Materials Science Journal* 6, 44-49. DOI: 10.2174/1874088X01206010044

Su, C. W., Yuan, Q. P., Gan, W. X., Huang, J. D., and Huang, Y. Y. (2013). "The research on wood fiber/stainless steel net electromagnetic shielding composite board," *Key Engineering Materials* 525, 437-440. DOI: 10.4028/www.scientific.net/KEM.525-526.437

Sun, G., C., Liu, Z., L., and Yao, K., L. (2000). "Influence of the constitutive parameters of helical chiral materials on the electromagnetic wave rotation," *Journal of Functional Materials* 31(1), 38-39. DOI: 10.3321/j.issn:1001-9731.2000.01.012

Wang, L. J., Li, J., and Liu, Y. X. (2005). "Surface characteristics of electroless nickel plated electromagnetic shielding wood veneer," *Journal of Forestry Research* 16(3), 233-236. DOI: 10.1007/BF02856822

Xu, Z., Huang, Y. A., Yang, Y., Shen, J., Tang, T., and Huang, R. (2010). "Dispersion of iron nano-particles on expanded graphite for the shielding of electromagnetic radiation," *Journal of Magnetism and Magnetic Materials* 322(20), 3084-3087. DOI: 10.1016/j.jmmm.2010.05.034

Yavuz, Ö., Ram, M. K., Aldissi, M., Poddar, P., and Srikanth, H. (2005). "Polypyrrole composites for shielding applications," *Synthetic Metals* 151(3), 211-217. DOI: 10.1016/j.synthmet.2005.05.011

Yu, X., and Shen, Z. (2009). "The electromagnetic shielding of Ni films deposited on cenosphere particles by magnetron sputtering method," *Journal of Magnetism and Magnetic Materials* 321(18), 2890-2895. DOI: 10.1016/j.jmmm.2009.04.040

Yuan, Q. P., Su, C. W., Huang, J. D., Gan, W. X., and Huang, Y. Y. (2013). "Process and analysis of electromagnetic shielding in composite laminated with electroless nickel-plated carbon fiber," *BioResources* 8(3), 4633-4646. DOI: 10.15376/biores.8.3.4633-4646

Yuan, Q. P., Lu, K. Y., and Fu, F. (2014). "Process and structure of electromagnetic shielding plywood composite laminated with carbon fiber paper," *The Open Materials Science Journal* 8, 99-107. DOI: 10.2174/1874088x01408010099

Yusoff, A. N., and Abdullah, M. H. (2004). "Microwave electromagnetic and absorption properties of some LiZn ferrites," *Magn. Magn. Mater* 269(2), 271-280. DOI: 10.1016/S0304-8853(03)00617-6

Zhang, X. Q., Liu, Y. X., and Li, J. (2004). "Wood fiber and iron wire netting composite MDF," *Journal of Northeast Forestry University* 32(5), 15-19. DOI: 10.13759/j.cnki.dlxb.2004.05.010

Zhao, F. C. (2001). "Development of electromagnetic shielding materials," *Development and Application of Materials* 16(5), 29-33. DOI: 10.3969/j.issn.1003-1545.2001.05.009

Zhao, J. J., Li, X. X., Guo, Y. X., and Ma, D. Y. (2014). "Highly exfoliated graphite prepared by two-step intercalation and its microstructure," *Ordnance Material Science and Engineering* 37(4), 4-8. DOI: 10.3788/OPE.20142205.1267

Article submitted: November 27, 2015; Peer review completed: February 6, 2016; Revised version received and accepted: April 9, 2016; Published: April 21, 2016.
DOI: 10.15376/biores.11.2.5083-5099